FEBS Letters 23717 (2000) 252–256 FEBS 23717

FEBS 23619

Correspondence

Does nitric oxide synthase catalyze the synthesis of superoxide?

Kai Y. Xu*

The characteristic function of all NOS isoforms, including neuronal NOS (nNOS), inducible NOS (iNOS), endothelial NOS (eNOS) and nNOSμ, is to catalyze the synthesis of $NO^{\bullet}$, a gaseous reactive radical that regulates important cellular functions (reviewed in [1]). This catalytic activity of NOS requires L-arginine and the binding of its coenzyme, reduced nicotinamide adenine dinucleotide phosphate (NADPH), and cofactors, such as flavin adenine dinucleotide (FAD), flavin mononucleotide (FMN), tetrahydrobiopterin (BH_4) and calmodulin (CaM). It has been reported that NOS not only produces $NO^{\bullet}$, but also functionally generates $O_2^{\bullet-}$ in the absence of L-arginine [2]. The question as to whether NOS catalyzes the synthesis of $O_2^{\bullet-}$ is fundamental to the understanding of the biological function of NOS and requires a rigorous reexamination. In the present study, it was found that NOS cofactors and NADPH induce non-specific $O_2^{\bullet-}$ radical generation. The evidence that a similar amount of $O_2^{\bullet-}$ was detected from all forms of NOS, including native, denatured, trypsin-digested and inhibitor-inactivated enzymes in the absence of L-arginine and the presence of NADPH and NOS cofactors, indicated that NOS does not catalyze $O_2^{\bullet-}$ radical formation. The nNOS was chosen for the following experiments because it has been highly purified ($>98\%$) and all of the NOS isoforms share the same catalytic function.

We first tested whether nNOS itself or the reaction buffer (50 mM Tris–HCl, pH 7.4) produces $O_2^{\bullet-}$ radicals. Electron paramagnetic resonance (EPR) spectroscopy was used to directly measure $O_2^{\bullet-}$ generation in the presence of 100 mM spin trap 5,5,-demethyl-1-pyrroline-1-oxide (DMPO). Fig. 1 indicates that neither the reaction buffer alone (Fig. 1A) nor with native nNOS (12 μg/ml) itself (Fig. 1B) showed any detectable $O_2^{\bullet-}$ radical signal. We next examined whether NOS coenzyme and cofactors generate $O_2^{\bullet-}$ radicals. The EPR spin-trap measurements reveal that a mixed signal, including DMPO-OOH, which represents $O_2^{\bullet-}$ consisting of a 1:1:1:1:1:1 sextet ($\alpha_N = 14.2$ G, $\alpha_H = 11.4$ G, $\alpha_{H'} = 1.2$ G) and a 1:2:2:1 quartet originating from the DMPO-OH ($\alpha_N = \alpha_H = 14.9$ G) for hydroxyl radical ($OH^{\bullet}$), were observed from a mixture of NADPH, FAD, FMN, BH_4 and CaM (Fig. 1C). Both DMPO-OOH and DMPO-OH adducts were completely inhibited by superoxide dismutase (SOD) suggesting that DMPO-OH is $O_2^{\bullet-}$-dependent (Fig. 1I,H). When native nNOS was mixed with NADPH, FAD, FMN, BH_4 and CaM, a similar amount of the mixed signal (DMPO-OOH and DMPO-OH) was detected (Fig. 1D) compared with the signal from the mixture of NADPH and nNOS cofactors (Fig. 1C). This result shows that highly purified native nNOS did not enhance the generation of $O_2^{\bullet-}$ radicals under the conditions used in Fig. 1C, suggesting that nNOS did not catalyze $O_2^{\bullet-}$ formation in the absence of L-arginine. To verify this observation, native nNOS was denatured by boiling at 100°C for 10 min prior to being mixed with NADPH and NOS cofactors. The EPR measurement showed that denatured nNOS did not abolish the mixed signals (Fig. 1E) and that the same amount of DMPO-OOH was observed again compared with Fig. 1C,D, suggesting that the $O_2^{\bullet-}$ radical seen from the reaction mixture is not a functional product of nNOS. To further confirm our results, native nNOS was digested by trypsin overnight, in order to destroy the three-dimensional structure of the enzyme, and then mixed with NADPH and NOS cofactors and subjected to the EPR measurement. The result shows that trypsin-digested nNOS did not alter the $O_2^{\bullet-}$ generation (Fig. 1F) compared with various conditions as shown in Fig. 1C,D,E. Furthermore, Fig. 1G shows that a similar amount of DMPO-OOH was also detected from inactivated nNOS in the presence of NOS inhibitors (L-NAME, TRIM, AMT and 7NI, 0.2 mM each) indicating that NADPH and NOS cofactor-induced $O_2^{\bullet-}$ radical generation is irrelevant to NOS catalytic function. Multiple inhibitors were used in order to reach maximum inactivation of the enzyme.

The simplest way to examine whether NOS functionally generates $O_2^{\bullet-}$ is to compare the $O_2^{\bullet-}$ radical generation in both native and denatured NOS enzyme systems. In the present study, similar amounts of $O_2^{\bullet-}$ radical production were detected from denatured nNOS (absence of catalytic activity and fully unfolded protein) compared with native nNOS (Fig. 1D,E,F). These facts clearly demonstrate that nNOS does not catalyze $O_2^{\bullet-}$ radical formation. While no enzymatic activity or $NO^{\bullet}$ generation was seen from boiled, trypsin-digested or inactivated nNOS enzymes under the same conditions as described in Fig. 1 (data not shown), $O_2^{\bullet-}$ radicals were formed (Fig. 1). These results underscore that the $O_2^{\bullet-}$ radical is not a catalytic product of nNOS. EPR spin trapping measurements provide direct evidence that NOS coenzyme and cofactors induce $O_2^{\bullet-}$ radical generation (Fig. 1C). These data suggest that complex chemical interactions among NADPH, FAD, FMN, BH_4 and CaM may be responsible for the $O_2^{\bullet-}$ formation. The DMPO-OH signal that coexisted with DMPO-OOH, was completely inhibited by SOD (Fig. 1H,I), an enzyme that specifically catalyzes removal of the $O_2^{\bullet-}$ radicals, [3] demonstrating that the DMPO-OH is $O_2^{\bullet-}$-dependent. Whether flavins could photosensitize the oxidation of NADPH with abundant $O_2^{\bullet-}$ to induce $O_2^{\bullet-}$-dependent $OH^{\bullet}$ generation [4], or DMPO-OH is solely decomposed from DMPO-OOH [5], remains to be determined. It has been reported that BH_4 generates $O_2^{\bullet-}$ through autooxidation,[6] and that FAD and FMN induce $O_2^{\bullet-}$ production [7]. The observations (Fig. 1C) reported here are consistent with those findings and further indicate that the $O_2^{\bullet-}$ radicals derived from NADPH and NOS cofactors are non-specific by-products, presumably due to the molecular autooxidation and interactions involving redox electron transfer.

The studies reported here demonstrate that NOS does not catalyze $O_2^{\bullet-}$ production and that NADPH and NOS cofactors induce $O_2^{\bullet-}$ generation. More detailed investigation of the chemical mechanisms of the $O_2^{\bullet-}$ generation from NOS coenzyme and cofactors, and of how NO regulates this $O_2^{\bullet-}$ formation in vivo, should increase our understanding of the biological function of NOS.

PII: S0014-5793(00)01589-1

Fig. 1. EPR spectra of $O_2^{\bullet -}$ generation in the presence of 100 mM DMPO under various conditions. Measurements were performed in a flat cell at room temperature. The spin trapping reagent DMPO (100 mM) was used and the integrated intensity of the DMPO-OOH and DMPO-OH adducts was monitored as a measure of the apparent amount of $O_2^{\bullet -}$ generation. The final concentrations for nNOS, NADPH, BH4, FAD, FMN, CaM and SOD were 12 μg/ml, 1 mM, 10 μM, 5 μM, 5 μM, 0.1 mg/ml and 1000 U/ml, respectively. A: 50 mM Tris–HCl buffer, pH 7.4. B: Native nNOS. C: A mixture of NADPH, BH_4, FAD, FMN, and CaM. D: (B) under condition (C). E: Boiled nNOS under condition (C). F: Trypsin-digested nNOS under condition (C). G: L-NAME+TRIM+AMT+7NI (0.2 mM each) under condition (D). H: SOD under condition (C). I: SOD under condition (G). Each data point represents five similar measurements. The EPR spectra were recorded immediately after the spin trap was added by using an IBM-Bruker ER 300 spectrometer operating at X-band with a transverse magnetic 110 cavity. The spectrometer settings were as follows: modulation frequency, 100 kHz; modulation amplitude, 1 G; scan time, 1 min; total acquisition time, 2 min; microwave power, 20 mW, and microwave frequency, 9.78 GHz.
←

Acknowledgements: I thank Dr. Anne Kagey-Sobotka, Dr. Irwin Fridovich, Dr. David Proud and Dr. Bradley J. Undem for their helpful suggestions and useful comments on the manuscript. This work was supported by a grant from The American Heart Association and by the US National Institute of Health grant HL-52175.

References

[1] Christopherson, K.S. and Bredt, D.S. (1997) J. Clin. Invest. 100, 2424–2429.
[2] Pou, S., Keaton, L., Surichamorn, W. and Rosen, G.M. (1999) J. Biol. Chem. 274, 9573–9580.
[3] Fridovich, I. (1995) Annu. Rev. Biochem. 64, 97–112.
[4] Zee, J.V.D., Krootjes, B.B.H., Chignell, C.F., Dubbelman, T.M.A.R. and Steveninck, J.V. (1993) Free Radic. Biol. Med. 14, 105–113.
[5] Finkelstein, E., Rosen, G.M. and Rauckman, E.J. (1981) Mol. Pharmacol. 21, 262–265.
[6] Mayer, B., Klatt, P., Werner, E.R. and Schmidt, K. (1995) J. Biol. Chem. 270, 655–659.
[7] Halliwell, B. and Gutteridge, J.M.C. (1985) Free Radicals in Biology and Medicine, Oxford University Press, New York.

*Fax: (1)-410-550 7480.
E-mail: kxu@jhmi.edu

Department of Medicine, Division of Cardiology, The Johns Hopkins Medical Institution, Hopkins Asthma and Allergy Center, 1A2, 5501 Hopkins Bayview Circle, Baltimore, MD 21224, USA

FEBS 23717

The disulphide bond arrangement in the major pepsin inhibitor PI-3 of *Ascaris suum*

Karen Girdwood, Colin Berry*

Proteins that inhibit aspartic proteinases are very rare in nature. However, the parasitic nematode *Ascaris suum* produces a protein, PI-3, that inhibits the aspartic proteinases pepsin, gastricsin and cathepsin E [1,2]. The 149-residue protein sequence of the mature PI-3 inhibitor (generated by removal of a signal peptide) was determined [3] and contains six cysteine residues, all of which were shown to be involved in disulphide bonding by Martzen et al. [3] who proposed the following disulphide pairings: Cys-13–Cys-59; Cys-48–Cys-66; Cys-79–Cys-146 (Fig. 1).

Subsequently, genes encoding homologues of PI-3 have been identified in other parasitic nematode species (*Onchocerca volvulus*, *Acanthocheilonema viteae*, *Brugia malayi* and *Dirofilaria immitis*) and within the genome of the free living nematode *Caenorhabditis elegans* (accession numbers P21250,

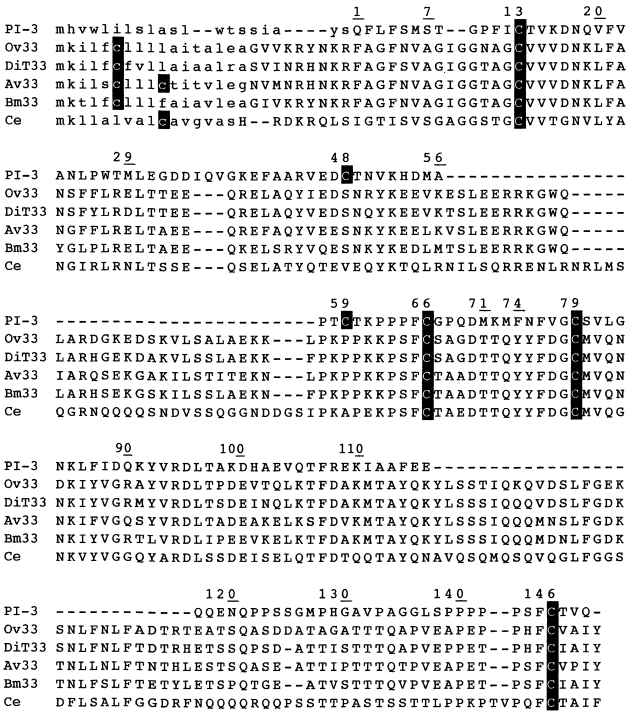

Fig. 1. PI-3 alignment. The sequence of the aspartic proteinase inhibitor from *A. suum* (PI-3) is aligned with homologues from *O. volvulus* (Ov33), *D. immitis* (DiT33), *A. viteae* (Av33), *B. malayi* (Bm33) and *C. elegans* (Ce). Hyphens indicate gaps introduced to optimise alignment. The numbering scheme follows that of Martzen et al. [3] and begins with the first residue of mature PI-3. Possible signal peptide sequences are shown in lowercase letters and cysteine residues are boxed.

S23229, L11001, U24180 and U20864 respectively). At least two of the proteins encoded by these genes (Ov33 from *O. volvulus* and DiT33 from *D. immitis*) appear to be able to inhibit aspartic proteinases such as pepsin [4].

Alignment of the amino acid sequences of these proteins with that of PI-3 (Fig. 1) indicates that the non-*Ascaris* proteins share greater identity with each other than with PI-3 (~20%), with a particular clustering of the molecules from *O. volvulus*, *A. viteae*, *D. immitis*, *B. malayi* and *D. immitis* (~75% identical). This is not unexpected since these five species all belong to the same taxonomic family (the Onchocercidae). Of greater significance may be the four Cys residues that are conserved in all of the sequences and the location of the major inserted sequences in each of the other proteins relative to PI-3.

Of the six cysteine residues present in PI-3, it is apparent that those at positions 13, 66, 79 and 146 (PI-3 numbering, Fig. 1) are conserved throughout the alignment whilst those at positions 48 and 59 are present only in PI-3. (Other cysteine residues found in the non-*Ascaris* sequences are within the putative signal peptide sequences.) If Cys-79 is paired with Cys-146 as suggested by Martzen et al. [3], then Cys-13 would need to be paired with Cys-66 in order to allow maximum consistency in the disulphide bonds throughout the proteins of this family. An S–S bond between residues 13–66 requires reconsideration of the 13–59 and 48–66 pairings assigned by Martzen et al. [3]. Following cleavage of non-reduced PI-3 by CNBr, these authors separated three fractions which consisted of (i) the N-terminal residues 1–6; (ii) two peptides consisting of residues 74–127 and 128–149 respectively (Fig. 1) that were disulphide linked, thus validating the Cys-79–Cys-146 pairing; and (iii) a peptide (residues 56–71 containing two Cys residues, 59 and 66; Fig. 2) which was connected by S–S bonds to each of two other peptides consisting of residues 7–29 (containing Cys-13), and 30–55 (containing Cys-48). With no further evidence, Martzen et al. [3] deduced that Cys-13 was linked to Cys-59 and Cys-48 to Cys-66 (Fig. 2a). Since Cys-48 and Cys-59 are not present in the PI-3 homologues, neither of these disulphide pairs would be conserved in the other family members. It would seem more valid, therefore, to propose that in PI-3, the pairing is just as likely between Cys-13–Cys-66, with the 48–59 pairing being present in the *Ascaris* sequence only. This model may also have structural implications. The first of the major insertions (31–39 residues long), in the non-*Ascaris* sequences is introduced in the sequence between the Cys-48 and Cys-59 residues. Since S–S bonds are commonly located on external loops, on or near the surface of most proteins, it is likely therefore that the inserted residues from the non-*Ascaris* sequences form an additional feature, possibly with a separate function, on the surface of these proteins. In contrast, in PI-3, which lacks this extended sequence, a disulphide linkage between Cys-48 and Cys-59 may serve to constrain the flanking regions to adopt a similar orientation.

It has been suggested that the *Ascaris* inhibitor may function to protect the nematode during passage through the host's digestive system or to evade immune responses [1,2]. However, the other nematodes listed in the legend to Fig. 1 do not pass through the stomach or intestine during their invasion of the host so that they do not encounter the gastric aspartic proteinases pepsin and gastricsin. Consequently, the ability to inhibit e.g. pepsin may be entirely fortuitous and of little physiological significance for the non-*Ascaris* proteins. Moreover, the presence of a homologue in the free living nematode *C. elegans* which has no requirement for evading gastric enzymes or immune defences may indicate a function for this family of proteins in the regulation of endogenous nematode aspartic proteinases, perhaps in a manner similar to that observed in yeast where the IA_3 inhibitor regulates an aspartic proteinase specifically that is also produced within the vacuole of the same yeast cell [5].

Acknowledgements: This study was supported by funding from a BBSRC studentship to K.G. and a Royal Society Research Fellowship to C.B.

References

[1] Valler, M.J., Kay, J., Aoyagi, T. and Dunn, B.M. (1985) J. Enzyme Inhib. 1, 77–82.
[2] Kageyama, T. (1998) Eur. J. Biochem. 253, 804–809.
[3] Martzen, M.R., McMullen, B.A., Smith, N.E., Fujikawa, K. and Peanasky, R.J. (1990) Biochemistry 29, 7366–7372.
[4] Girdwood, K. (1999) Aspartic proteinases and aspartic proteinase inhibitors from parasitic nematodes, PhD thesis, University of Wales, Cardiff.
[5] Li, M., Phylip, L.H., Lees, W.E., Winther, J.R., Dunn, B.M., Wlodawer, A., Kay, J. and Gustchina, A. (2000) Nat. Struct. Biol. 7, 113–117.

*Corresponding author.
E-mail: berry@cf.ac.uk

Cardiff School of Biosciences, Cardiff University, P.O. Box 911, Cardiff CF10 3US, Wales, UK

FEBS 23731

Reported channel formation by prion protein fragment 106–126 in planar lipid bilayers cannot be reproduced

Maria Manunta[a], Beat Kunz[b], Erika Sandmeier[b], Philipp Christen[b,*], Hansgeorg Schindler[a]

The normal prion protein is converted by an as yet unknown mechanism into its infectious scrapie form (PrP^{Sc}). The prion protein fragment 106–126 (PrP106–126) has been reported in numerous publications to elicit several effects of prion pathology, i.e. to be toxic to cultured neurons and to support the proliferation of glial cells and microglia ([1] and references cited therein). PrP106–126 is part of the NH_2-terminal flexible tail (residues 23–126) of the full-length murine prion protein with total 231 residues. Besides accumulation of PrP^{Sc} in the brain, neuronal vacuolation is observed suggesting plasma membrane dysfunction. PrP106–126 was reported to form ion channels in artificial planar lipid bilayers. These channels were described to be freely permeable for common physiological cations and chloride ions and their formation to be significantly enhanced if 'aged' peptide was used [2]. We tried to reproduce this channel-forming effect in order to test whether it correlated with the slow spontaneous deamidation of PrP106–126 [3].

In a first set of experiments, the prion peptide PrP106–126 with the sequence of H-KTNMKHMAGAAAAGAVVGG-LG-OH (purchased from Chiron, Australia, with a purity higher than 95%) was examined for possible channel-forming or ionophoric activity at the conditions for which ion channel activity had previously been reported [2]. Prp106–126, however, did not show any effect on the electrical properties of planar lipid bilayers when using the black lipid membrane (BLM) technique (for details, see Table 1). We found not even the least indication for channel events or any conductance in excess over the bare lipid membrane conductance of ~1 pS, for peptide concentrations of up to 100 μM (*cis* side) and for a total recording time of 40 min. The protocol included voltage application of up to 100 mV of either polarity, in fast alternation or in steady application, and with resting periods at zero voltage. These settings comprised any known voltage-dependent channel activation conditions.

A second set of experiments addressed the difficulty of verifying a negative finding by applying a more direct and more quantitative test for ionophoric activity of the peptide. For this purpose, we employed a strategy of forming lipid bilayers from lipid/peptide vesicles (septum-supported, vesicle-derived bilayer (SVB) technique [5]) so that the peptide was already present in the bilayer upon and after its formation at a defined molar ratio, adjusted to 100–500 lipid molecules per peptide molecule (for details, see Table 1). The SVB technique thus circumvents the insertion step of the peptide from the aqueous phase into preformed bilayers as necessary in the BLM technique. For any voltage treatment, the electrical properties of these peptide-containing membranes were identical to those of the bare lipid membrane. Soybean lipid (SBL) is probably the most often used standard lipid mixture for ion channel studies. SBL yields very stable bilayers which, due to the particular mixture of various lipids, provide an environment well suited for observing reproducible activities of incorporated ion channel-forming proteins. The absence of any modifying effect of the peptide, irrespective of the mode of bilayer formation (BLM or SVB technique) and of peptide addition used (to the bath or integrated at high density in SBL bilayers, respectively), leaves no doubt that formation of an ion channel or any ionophoric or lytic activity is not a characteristic feature of the prion peptide.

In addition to authentic PrP106–126 (with Asn-108), we tested whether PrP106–126 aged during 300 days at 37°C and the two synthetic deamidated isoforms PrP106–126 (L-

Table 1
Experimental conditions for studying lipid bilayers in the presence of prion peptides

Bilayer technique	Lipid composition	Prion peptide	Addition of peptide to bath (μM)	Peptide in lipid bilayer (mol %)	Total time of a single record (min)
BLM[a]	PE/PS/PC	PrP106–126	100	–	40
SVB[b]	SBL	–	–	–	30
SVB	SBL	PrP106–126	–	0.2–1	90
SVB	SBL	PrP106–126	100	0.2–1	68
SVB	SBL	PrP106–126 (aged)	–	0.2–1	32
SVB	SBL	PrP106–126 (L-isoAsp)	–	0.2–1	100
SVB	SBL	PrP106–126 (L-isoAsp)	100	0.2–1	26
SVB	SBL	PrP106–126 (L-Asp)	–	0.2–1	40

The bilayer apparatus was set up as previously described [5]; the membrane was formed across a 100-μm hole in a 12 μm thick Teflon septum. Total time of a single record specifies the electronically recorded time; the total analysis time was longer.

[a]BLM technique: the lipid bilayer was formed from a mixture of L-α-phosphatidylethanolamine (PE):L-α-phosphatidylserine (PS):L-α-phosphatidylcholine (PC) in weight ratios of 5:4:1, dissolved in decane at total 50 mg/ml. PrP106–126 was added to the preformed BLMs in the *cis* compartment to a final concentration of 100 μM as in the original report on Ca^{2+} channel formation [2]. Both chambers were filled with 100 mM sodium phosphate pH 7.4; the *cis* compartment contained 1 mM $CaCl_2$ in addition.

[b]SVB technique: the bilayer was formed by apposition of two vesicle-derived monolayers across a hole (diameter 100 μm) in a 12 μm thick Teflon septum. This procedure yielded solvent-free bilayers with specific capacitance values of 0.8 μF/cm^2 and, in contrast to BLMs, with defined peptide concentrations. Each chamber contained 1 ml of 1 M NaC1, 10 mM HEPES, pH 7.4. Thin films of 20 mg SBL without and with peptide (molar ratios of 100–500 of SBL/peptide, corresponding to 10^8 and 2×10^7 peptide molecules per bilayer, respectively) were dried under argon in a round flask and suspended in 15 ml 150 mM NaCl, 10 mM HEPES, pH 7.4 using mild agitation by rolling glass beads for 30 min. The salt concentration was then adjusted to 1 M NaCl yielding suspensions (1 mg/ml) of SBL vesicles or SBL/peptide vesicles. For bilayer formation from these vesicles, symmetrical conditions were used, i.e. both monolayers of the bilayers formed were derived from the same vesicle preparation. The molar ratio of lipid to peptide is maintained during bilayer formation.

Asp-108) or PrP106–126 (L-isoAsp-108), corresponding to the main derivatives generated during the aging process [3] induce the formation of ion channels. Table 1 provides a synopsis of these and the foregoing studies. In no instance was there any effect either of authentic PrP106–126 or of aged PrP106–126 and the two synthetic isoforms on the electrical properties of the lipid bilayers.

Our findings contrast with the previous report by Lin and coworkers [2]. Even under quite stringent conditions we were unable to observe any changes of membrane conductance by the prion peptide and its deamidated isoforms. The present results coincide with the recent findings that in our hands PrP106–126 was not able to induce neuronal cell death [4].

References

[1] Brown, D.R. (2000) Mol. Cell. Neurosci. 15, 66–78.
[2] Lin, M.C., Mirzabekov, T. and Kagan, B.L. (1997) J. Biol. Chem. 272, 44–47.
[3] Sandmeier, E., Hunziker, P., Kunz, B., Sack, R. and Christen, P. (1999) Biochem. Biophys. Res. Commun. 261, 578–583.
[4] Kunz, B., Sandmeier, E. and Christen, P. (1999) FEBS Lett. 458, 65–68.
[5] Schindler, H. (1989) Methods Enzymol. 171, 225–253.

*Corresponding author. Fax: (41)-1-635 5907.
E-mail: christen@biocfebs.unizh.ch

[a] *Institute for Biophysics, University of Linz, Altenberger Strasse 69, A-4040 Linz, Austria*
[b] *Biochemisches Institut, Universität Zürich, Winterthurerstrasse 190, CH-8057 Zurich, Switzerland*